

# CARBON BUDGET BALANCE AND INFLUENCING FACTORS IN THE YELLOW RIVER BASIN OF CHINA

WANG, S.<sup>1</sup> – LI, D.<sup>1</sup> – LI, X. J.<sup>2</sup> – LI, L. F.<sup>1</sup> – LI, Q.<sup>1,3</sup> – WANG, J. F.<sup>1\*</sup>

<sup>1</sup>*School of Geographical Science, Shanxi Normal University, Taiyuan 030031, P. R. China*

<sup>2</sup>*Department of Resources and Environmental Engineering, Shandong Agricultural and Engineering University, Jinan 250100, P. R. China*

<sup>3</sup>*Institute of Geographical Sciences, Hebei Academy of Sciences, Hebei Technology Innovation Center for Geographic Information Application, Shijiazhuang 050011, P. R. China*

*\*Corresponding author*

*e-mail: wangjinfeng@sxnu.edu.cn*

(Received 16<sup>th</sup> Nov 2024; accepted 5<sup>th</sup> Feb 2025)

**Abstract.** Focusing on the carbon budget balance in the context of global change, this study examines the carbon budget balance in the Yellow River Basin of China in the context of global change, using various methods to explore the driving mechanisms and predict net carbon emissions under different scenarios for 2030. From 2005 to 2020, direct carbon emissions in the Yellow River Basin decreased, carbon sink areas expanded, and net carbon emissions growth slowed down. Carbon emissions are mainly influenced by energy economy, with the effect of natural factors enhancing over time. The forecast results show that carbon emission under the ecological protection scenario in 2030 is  $12.63 \times 10^8$  t, which is 97.08% of the natural development scenario, and 95.61% of the urban expansion scenario. Therefore, controlling the expansion of construction land and high energy consumption, optimizing land use structure, and strengthening ecological land protection are recommended. The government should enhance low-carbon regulation of national land use and coordinate supporting policies to achieve carbon balance. This study has scientific reference significance for low-carbon and green development in resource-based areas with high energy consumption.

**Keywords:** *carbon budget, CO<sub>2</sub> emission, geographic detector, primary function-oriented zoning, Yellow River Basin*

## Introduction

Since the Industrial Revolution, the widespread use of coal, oil and other fossil fuels has led to substantial greenhouse gas emissions, driving global climate change characterized by rising temperatures and frequent extreme climatic events such as droughts and floods. This has posed significant challenges to human survival and socio-economic development and has also become a global concern (Ploeg and Withagen, 2012; Hussin et al., 2021). The Sixth Assessment Report by the United Nations Intergovernmental Panel on Climate Change (IPCC) highlights that the average global temperature increased by 1.09°C between 2011 and 2020 compared to the late 19th century, with industrialization being a significant contributing factor (IPCC, 2021; Wang et al., 2023). On June 30, 2015, China submitted the 'Strengthening Action on Climate Change – China's Nationally Determined Contribution to the United Nations, which proposed China's climate change targets for 2030, aiming to reduce CO<sub>2</sub> emission intensity by 60%-65% based on the level in 2005 (Strengthening Action on Climate Change, 2015; Xu et al., 2022). As a key participant in global climate governance, China

strives to achieve carbon peak around 2030 and carbon neutrality before 2060 (Xi, 2020), reflecting its responsibility and commitment.

The land is the complex syntheses between human activities and ecological environment, serving as the significant carbon source and sink. As an indispensable domain for human survival and development, the anthropogenic activities disrupt the natural carbon cycle, resulting in substantial increase of atmospheric greenhouse gas concentrations (Ma and Wang, 2015; Ran et al., 2023). LULC change is the second largest dedicator to CO<sub>2</sub> emissions following fossil fuel burning, making up 1/3 of global CO<sub>2</sub> emissions from 1850 to 2017 (Zhao et al., 2023). The carbon budget serves as the crucial metric for assessing the carbon flux within different earth system components (Quéré et al., 2018), making it the focus of global climate change research and a significant aspect of low-carbon and green development. Extensive investigations have been conducted on carbon budget accounting (Xia and Yang, 2022; Wang et al., 2023), carbon compensation (Li et al., 2023), influencing factors (Chang et al., 2022) and land use structure (Fan et al., 2018). Jayakrishnan et al. (2022) determined that land use accounted for over 40% of the total CO<sub>2</sub> emissions. By conducting an analysis of spatial disparities in CO<sub>2</sub> emissions within the Amazon basin, Gatti et al. (2021) deduced that deforestation and fire emerged as the primary factors contributing to the escalation of regional CO<sub>2</sub> emissions in the Amazon River Basin. Assis et al. (2022) investigated the impact factors on Amazon forest degradation and predicted the potential effects of future CO<sub>2</sub> emission scenarios on carbon balance. Chinese scholars have examined the carbon budget from diverse perspectives, encompassing scales, objects, content and methodologies. Based on the DMSP-OLS night light data and CO<sub>2</sub> emission statistics, Pan et al. (2021) observed consistent annual increase carbon footprint and carbon deficit in China from 2000 to 2013, and the spatial distribution was low in the south and high in the north. Since 1993, CO<sub>2</sub> emissions from LULC has emerged as the hot topic in China, revealing that factors such as land use type, mode, intensity and structure exert direct or indirect influences on the CO<sub>2</sub> emissions and absorption processes of terrestrial ecosystems and atmosphere (Zhao et al., 2016; Huang et al., 2021). With the development in observation and simulation technology, the carbon budget calculation methodology has evolved from measuring atmospheric CO<sub>2</sub> concentration to employing inversion techniques (Jin et al., 2023). The common carbon accounting inventory of IPCC has been highly recognized for its robust applicability and has been extensively utilized in multi-spatial scale research (Aleinikovas et al., 2018; Zhang et al., 2018; Mi et al., 2019).

The Yellow River Basin is the strategic region and the crucial ecological functional area in China high-quality economic development, playing an indispensable role in attaining CO<sub>2</sub> emission reduction. As the crucial energy hub, the current energy structure of the Yellow River Basin is dominated by fossil fuels, with dense coal chemical industries contributing to increase CO<sub>2</sub> emissions and exert significant pressure on ecological environment. The Yellow River Basin is characterized by high energy consumption, pollution and emissions, with low energy utilization efficiency and severe ecological environment degradation. At present, the socio-economic development across the upper, middle and lower reaches of the Yellow River presents significant disparities and is undergoing profound energy structure and socio-economic transformation, resulting in intensified emission reduction pressure. Land resources play a pivotal role in the ecosystem and serve as a significant driver of CO<sub>2</sub> emissions. The preservation of the carbon balance within the ecosystem, coupled with emission reduction and energy conservation, is intricately linked to fostering. Reducing CO<sub>2</sub> emissions and maintaining

ecosystem carbon balance are important to high-quality development in the Yellow River Basin.

So as to ensure the ecological security of the Yellow River and its surrounding areas, China has implemented the "major function-oriented zoning plan". Considering landform, climatic conditions, resource endowment, development potential and ecological environment, the Yellow River Basin is categorized into optimized, key, restricted and prohibited development zones (Fan et al., 2010), aiming to achieve sustainable development and ecological civilization construction (Huang and Pan, 2020). The ecologically fragile Yellow River Basin exhibits evident spatial disparities in socio-economic development level, and resource and environmental carrying capacity, with distinct CO<sub>2</sub> emission reduction tasks in vary major function-oriented zones (Fan, 2015). However, the spatial heterogeneity and correlation of carbon budget balance have been overlooked in previous studies, leading to the lack of targeted CO<sub>2</sub> emission reduction measures and compensation mechanisms. Therefore, the study strives to: (1) analyze carbon budget balance by quantifying direct CO<sub>2</sub> emissions, indirect CO<sub>2</sub> emissions and LULC carbon carrying capacity. (2) investigate the effect of social and natural factors on CO<sub>2</sub> emissions by the geographical detector method. (3) project CO<sub>2</sub> emissions trend and put forward low-carbon development countermeasures by setting natural development, urban expansion and ecological protection scenarios. This study will provide crucial scientific references for achieving global carbon budget equilibrium and offer theoretical foundation and support for the Chinese government to design CO<sub>2</sub> emission reduction plans and accomplish high-quality development goals in the Yellow River Basin.

### ***Study area***

The Yellow River (31°42'N~45°42'N, 89°35'E~122°17'E, *Fig. 1*) serves as the crucial ecological security barrier and an economically significant region in China, encompassing the total area of  $75.24 \times 10^4 \text{ km}^2$ . It exercises jurisdiction eight provinces and regions: Qinghai, Gansu, Ningxia, Inner Mongolia, Shaanxi, Shanxi, Henan and Shandong, which comprises of 91 municipal administrative units along with 739 districts and counties. Referring to the primary function-oriented zoning in 2010 (Fan et al., 2010), the Yellow River Basin is categorized into eight functional zones: National Key Development Prioritized Zone (NKDPZ), Provincial Key Development Prioritized Zone (PKDPZ), National Development Optimized Zone (NDOZ), Provincial Development Optimized Zone (PDOZ), National Major Grain Producing Zone (NMGPZ), Provincial Major Grain Producing Zone (PMGPZ), National Key Ecological Function Zone (NKEFZ), Provincial Key Ecological Function Zone (PKEFZ). The land use is predominantly comprised of grassland and unused land, accounting for 45% and 27% respectively in 2020. The basin is abundant in natural resources, particularly mineral resources, and serves as the primary source for energy consumption and supply in China, also the pivotal region for CO<sub>2</sub> emissions resulting from energy consumption (Yang and Zhen, 2023). In 2020, energy consumption in the Yellow River Basin reached  $13.88 \times 10^8 \text{ t}$ , accounting for 29.9% and 35.1% of total energy consumption and CO<sub>2</sub> emissions, respectively. The abundant fossil energy drives rapid economic development in the Yellow River Basin; but also imposes significant challenges for CO<sub>2</sub> emission reduction. The CO<sub>2</sub> emission reduction in the Yellow River Basin plays the pivotal role in achieving "carbon neutrality" and "carbon peak" of China, which will lead the new social and economic development within the basin.

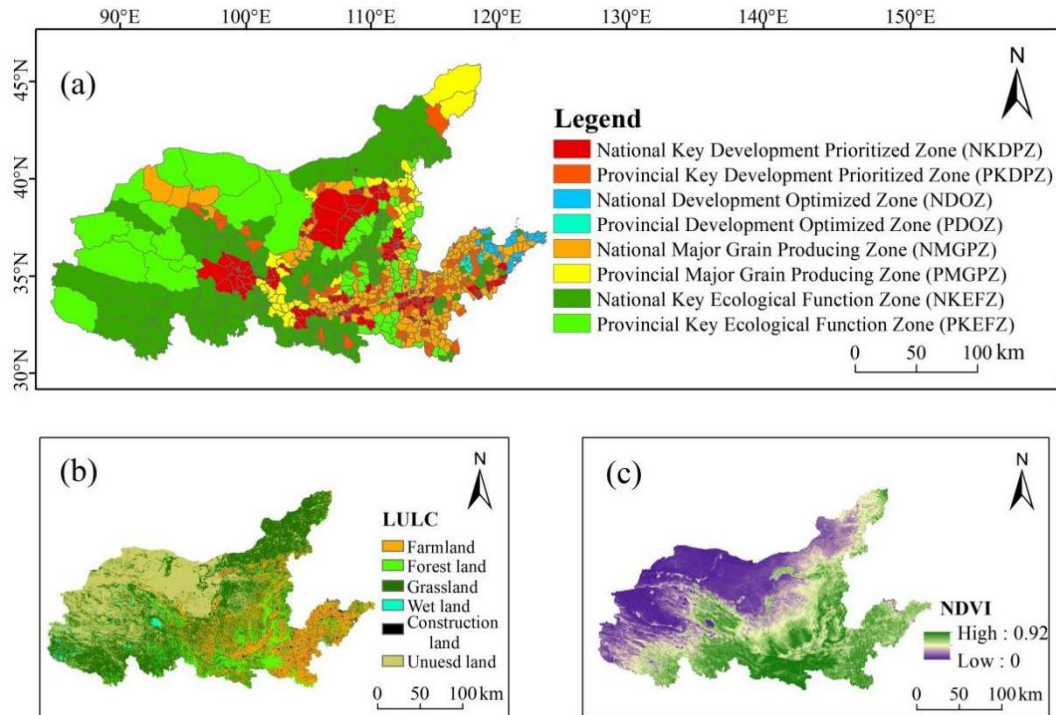


**Figure 1.** (a) Primary function-oriented zones of Yellow River Basin (Fan et al., 2010, <https://bzdt.ch.mnr.gov.cn/>), (b) LULC (Land-use/land-cover, LULC, <https://www.resdc.cn/Default.aspx>) and (c) NDVI (Normalized Difference Vegetation Index, NDVI, <https://www.resdc.cn/Default.aspx>) spatial pattern

## Materials and methods

### Data sources

The data primarily consist of two categories: remote sensing data and socio-economic data, covering the time span from 2000 to 2020. Remote sensing data include LULC, NDVI and DEM (Digital Elevation Model, DEM). Socio-economic data include major function-oriented zoning, major roads and railways, GDP (Gross domestic product, GDP), population and energy. The data classification is shown in the *Table 1*.

**Table 1.** Data classification

Data	Classification	Type	Spatial resolution	Data source
Remote sensing data	LULC	Grid	1km×1km	Data Center for Resources and Environmental Sciences, Chinese Academy of Sciences Geospatial data cloud
	NDVI	Grid	1km×1km	
	DEM	Grid	1km×1km	
Socio-economic data	Major function-oriented zoning	Vector	—	China government network
	Main highway	Vector	—	National basic geographic information System
	Main railway	Vector	—	
	GDP	Data table	—	China county Statistical Yearbook and regional statistical Bulletin
	Population	Data table	—	China Energy Statistical Yearbook
Source of energy	Data table	—		

## Methods

### Carbon budget measurement methods

The accounting inventory is developed on the basis of the IPCC National Greenhouse Gas Inventories, and the carbon budget is determined using the following calculation formula:

$$CB = DCE + ICE - CS \quad (\text{Eq.1})$$

where,  $CB$  is carbon budget,  $DCE$  is direct  $\text{CO}_2$  emission,  $ICE$  is indirect  $\text{CO}_2$  emission,  $CS$  is carbon sink (carbon carrying capacity).

$DCE$  refers to the loss of LULC carbon storage, which is counted using the carbon module of InVEST model, including above-ground biological carbon density, underground biological carbon density and soil organic matter carbon pool density.

$$C_{SP} = 3.3968 \times P + 3996.1 \quad (\text{Eq.2})$$

$$C_{BP} = 6.7981e^{0.00541P} \quad (\text{Eq.3})$$

$$C_{BT} = 28 \times T + 398 \quad (\text{Eq.4})$$

where,  $C_{SP}$  is the soil carbon density;  $C_{BP}$  and  $C_{BT}$  are the above-ground and underground biological carbon density, respectively;  $P$  is the annual precipitation;  $T$  is the annual average temperature. The annual average temperature and precipitation for China ( $7.15^\circ\text{C}/673.9\text{mm}$ ) and Yellow River Basin ( $6.86^\circ\text{C}/362.09\text{mm}$ ) are used to calculate the correction coefficient (Giardina and Ryan, 2000; Chen et al., 2007; Alam et al., 2013).

$$K_B = K_{BP} \times K_{BT} = \frac{C'_{BP}}{C''_{BP}} \times \frac{C'_{BT}}{C''_{BT}} \quad (\text{Eq.5})$$

$$K_S = \frac{C'_{SP}}{C''_{SP}} \quad (\text{Eq.6})$$

where,  $K_B$  and  $K_S$  are the correction coefficients of biological and soil carbon density, respectively;  $K_{BP}$  and  $K_{BT}$  are the correction coefficients of the above-ground and underground biological carbon density, respectively;  $C'_{BP}$ ,  $C'_{BT}$  and  $C'_{SP}$  are above-ground biological carbon density, underground biological carbon density and soil carbon density of the Yellow River Basin, respectively;  $C''_{BP}$ ,  $C''_{BT}$  and  $C''_{SP}$  are above-ground biological carbon density, underground biological carbon density and soil carbon density of China, respectively. The carbon density of the Yellow River Basin can be calculated by multiplying the carbon density data of China with above correction coefficients (Table 2).

$ICE$  is primarily derived from construction land, and industry and the burning of fossil fuels are major emission sources. To calculate indirect  $\text{CO}_2$  emissions, nine energy sources are considered, namely coke, coal, kerosene, diesel, crude oil, gasoline, natural gas, fuel oil and electricity. The calculation formula is as follows (Zheng and Wen, 2010; Buendia et al., 2006; Zhou et al., 2019):

$$ICE = \sum_{i=1}^9 E_{ti} = \sum_{i=1}^9 (E_{ni} \times \theta_i \times f_i) \quad (\text{Eq.7})$$

where,  $ICE$  represents the total  $CO_2$  emissions from the terminal consumption of fossil fuels;  $E_{ti}$  represents the  $CO_2$  emissions from the terminal consumption of Class  $i$  fossil energy;  $E_{ni}$  represents final consumption of all types of fossil energy;  $\theta_i$  represents the converted criteria coal coefficient of various fossil energy sources;  $f_i$  represents the  $CO_2$  emission coefficient of each energy source.

**Table 2.** Carbon density in the Yellow River Basin ( $t\text{ hm}^{-2}$ )

Land use	Above-ground biomass	Underground biomass	Soil
Farmland	1.02	14.44	69.75
Forest land	7.58	20.76	90.12
Grassland	6.71	15.48	77.23
Wet land	0	0	11.63
Construction land	0.45	0	64.85
Unused land	0.233	0	26.11

$CS$  refers to the quantity of  $CO_2$  sequestered by regional vegetation. Agricultural production predominantly relies on  $CO_2$  emissions, while cultivated land is not included in the accounting scope of carbon sink. The carbon sink capability of forest land, grassland and water area was quantified in this study. The calculation formula employed is as follows:

$$CS = \sum_{j=1}^3 L_j \times \theta_j \quad (\text{Eq.8})$$

where,  $L_j$  is the area of Class  $j$  land use type;  $\theta_j$  is the carbon sequestration rate per unit area (Walsh, 2001).

#### Geographic detector

The Geodetector is the statistical approach utilized for detecting spatial differentiation and identifying the underlying driving factors, enabling the analysis of multifactor interactions across diverse phenomena. Geographic detector possesses the advantages of detecting both quantitative and qualitative data, thereby effectively mitigating the issue of subjective factors influencing multi-factor weights. The method comprises factor detector, risk detector, interaction detector and ecological detector (Wang et al., 2010; Wang and Hu, 2012; Wang and Xu, 2017). The factor detection is employed to discern the spatial disparity of object  $y$ . The parameter  $q$  ( $0 < q < 1$ ) quantifies the explanatory power of factor  $x$ . Interaction detection is utilized to ascertain whether the joint influences of two factors ( $x_1$  and  $x_2$ ) on  $y$  are interrelated or independent. The single factor influence on  $y$  is denoted as  $q(x_1)$  and  $q(x_2)$ , while the interaction between the two factors is denoted as  $q(x_1 \cap x_2)$ . The interaction type and decision basis are presented in Table 3.

#### CA-Markov model

The CA-Markov model integrates the strengths of Markov model time series prediction and CA model spatial simulation (Syphard et al., 2005; Caute and Lawrence, 2017; Zhou et al., 2020). The cellular transformation rule designates the year 2000 as the initial point for land use data, while 2015 serves as the termination year. Both the age

interval and predicted age are set at 15 years, with the tolerance of 0.15. The Kappa coefficient between measured and simulated land use in 2015 was 0.83, indicating the high reliability. Based on 2015, LULC in 2030 is predicted under different scenarios: (1) Natural development scenario: This scenario is based on the transfer matrix from 2000 to 2015, with land use conversion probability matrix unchanging. (2) Urban expansion scenario: The conversion probability from cultivated land, forest land, grassland and unused land to construction land increased by 5%, 1%, 2% and 4% in 2030. In the formulation of the suitability map, the most suitable location of industries and mines should be set within 800 m of the main railways and highways. (3) Ecological protection scenario: In accordance with the national ecological policy, the transfer probability of cultivated land to forest land was increased by 5%, and the transfer probability of cultivated land, forest land, grassland and unused land to construction land was reduced by 4%, 2%, 1% and 1%. The water body is considered as restrictive factor, and the conversion to any land category is strictly prohibited.

**Table 3.** Factor interaction type and judgment basis

Judgment basis	Interaction type
$q(x_1 \cap x_2) < \min(q(x_1), q(x_2))$	Reduction of nonlinearity
$q(x_1 \cap x_2) < \max(q(x_1), q(x_2))$	Two-factor enhancement
$\min(q(x_1), q(x_2)) < q(x_1 \cap x_2) < \max(q(x_1), q(x_2))$	Nonlinear attenuation of single factor
$q(x_1 \cap x_2) > q(x_1) + q(x_2)$	Enhancement of nonlinearity
$q(x_1 \cap x_2) = q(x_1) + q(x_2)$	Mutual independence of factors

## Results

### *Spatial and temporal distribution of carbon budget in the Yellow River Basin*

#### *Direct CO<sub>2</sub> emissions*

The spatial pattern of direct CO<sub>2</sub> emissions in the Yellow River Basin from 2005 to 2020 are depicted in Fig. 2. The direct CO<sub>2</sub> emissions in 2005 amounted to  $0.18 \times 10^8$  t, with 57.61% of the counties being carbon sources. Among them, 78.87% originated from NKDPZ and NKEFZ, which were the primary contributors to direct CO<sub>2</sub> emissions within the Yellow River Basin. The change in LULC mode has resulted in the negative CO<sub>2</sub> emission in PMGPZ, thereby enhancing the ecological carbon sequestration capacity. In 2010, direct CO<sub>2</sub> emissions amounted to  $-0.09 \times 10^8$  t. With the exception of PKDPZ and development optimized zone, all other major function-oriented zones exhibited negative CO<sub>2</sub> emissions, indicating the well-developed carbon storage over the past five years. The direct CO<sub>2</sub> emissions amounted to  $0.03 \times 10^8$  t in 2015, with approximately 73.37% of the counties being carbon sources. Except for NKDPZ and PKEFZ, CO<sub>2</sub> emissions of other major function-oriented areas exceeded zero. Due to the conversion of the substantial amount of ecological land into construction land, NMGPZ experienced significant increase in CO<sub>2</sub> emissions by  $0.02 \times 10^8$  t. The CO<sub>2</sub> emissions of NKDPZ and PKEFZ were  $-2 \times 10^4$  t and  $-5 \times 10^4$  t, respectively, indicating the weak carbon sequestration effect. The direct CO<sub>2</sub> emissions increased significantly in 2020, reaching  $1.01 \times 10^8$  t, and PKEFZ became the highest CO<sub>2</sub> emission zone. Furthermore, approximately 30% of anthropogenic greenhouse gas emissions originate from agricultural land, and  $1.2 \times 10^4$  km<sup>2</sup> grassland has been transformed to agricultural land resulting in elevated CO<sub>2</sub> emissions of NDOZ.

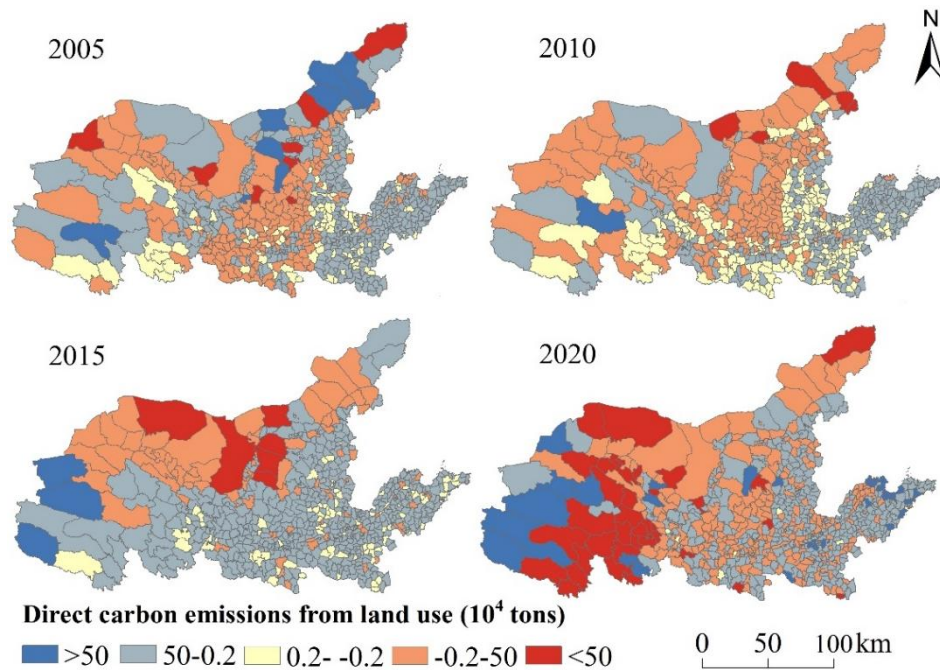


**Figure 2.** Spatial distribution of direct CO<sub>2</sub> emissions from land use in 2005, 2010, 2015 and 2020

#### Indirect CO<sub>2</sub> emissions

The statistical results of indirect CO<sub>2</sub> emissions in the Yellow River Basin are shown in Table 4. In 2005, 2010, 2015 and 2020, the indirect CO<sub>2</sub> emissions in the Yellow River Basin were 6.77, 10.47, 12.81 and 13.74×10<sup>8</sup> t, respectively, showing an obvious upward trend. The change trends vary across different functional areas. The indirect CO<sub>2</sub> emissions of key development prioritized zones, NMGPZ and key ecological function zones exhibited an upward trend, whereas the development optimized zones and PMGPZ both reached the peak in 2015, and then showed slight decline, with reduction rate of 0.01%, 2.36%, and 3.18%, respectively.

**Table 4.** Indirect CO<sub>2</sub> emissions and contribution rates of energy consumption in 2005, 2010, 2015 and 2020

Year	Functional zone	NKDPZ	PKDPZ	NDOZ	PDOZ	NMGPZ	PMGPZ	NKEFZ	PKEFZ
2005	CO <sub>2</sub> emission/10 <sup>8</sup> t	1.94	1.17	0.74	0.39	1.61	0.07	0.63	0.22
	Contribution rate/%	28.66	17.24	10.97	5.73	23.78	1.00	9.29	3.32
2010	CO <sub>2</sub> emission/10 <sup>8</sup> t	3.36	1.57	1.04	0.59	2.34	0.16	0.84	0.57
	Contribution rate/%	32.08	14.98	9.95	5.66	22.37	1.49	8.01	5.47
2015	CO <sub>2</sub> emission/10 <sup>8</sup> t	4.01	1.88	1.44	0.69	2.92	0.19	1.02	0.65
	Contribution rate/%	31.28	14.72	11.23	5.39	22.83	1.54	7.97	5.04
2020	CO <sub>2</sub> emission/10 <sup>8</sup> t	4.11	1.89	1.44	0.67	3.67	0.19	1.02	0.73
	Contribution rate/%	4.11	13.80	10.46	4.90	26.68	1.39	7.49	5.35

The spatial trend of indirect CO<sub>2</sub> emissions in the Yellow River Basin is illustrated in Fig. 3. The industrial development in the Yellow River Basin was sluggish in 2005, the number of counties with low CO<sub>2</sub> emissions (<70×10<sup>4</sup> t) was dominant, and the CO<sub>2</sub> emissions in the western were obvious lower than the eastern. The CO<sub>2</sub> emissions in all regions and counties presented varying increase degrees in 2010, especially in central Inner Mongolia and certain parts of Qinghai. The overall CO<sub>2</sub> emissions showed upward trend in 2015, the number of districts and counties with CO<sub>2</sub> emissions surpassing 200×10<sup>4</sup> t increased significantly. Although PDOZ occupied only 0.33%, the CO<sub>2</sub> emissions increased to 5.38%. In 2020, CO<sub>2</sub> emissions from energy consumption reached the maximum, the regions with CO<sub>2</sub> emissions below 10×10<sup>4</sup> t were only distributed in Yushu and Guoluo of NKEFZ. Although CO<sub>2</sub> emissions increased in NKDPZ, PKDPZ and NKEFZ compared to 2015, the CO<sub>2</sub> emission contribution rates have decreased by 1.35%, 0.92% and 0.48%, respectively.

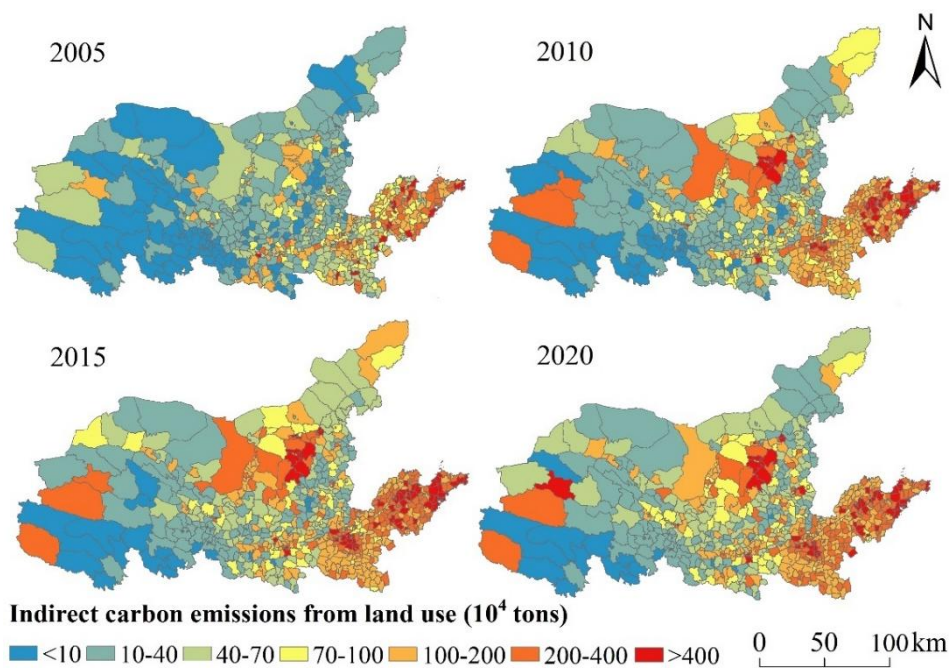


**Figure 3.** Spatial distribution of indirect CO<sub>2</sub> emissions from land use in 2005, 2010, 2015 and 2020

### Carbon carrying capacity (carbon sink)

The average annual carbon sequestration in the Yellow River Basin from 2005 to 2020 was  $1.85 \times 10^8$  t. The carbon sink of water area, grassland, and forest land respectively increases by 15.18%, 4.18% and 2.04%. For different major function-oriented areas, the carbon sink of PMGPZ was basically stable at  $0.15 \times 10^8$  t from 2005 to 2015, with an accelerated growth rate thereafter. However, the contribution rate of carbon sink slightly declined from 7.97% in 2005 to 7.93% in 2020. NKEFZ is mainly grassland and forest land, exhibiting the highest carbon sequestration effect, with the contribution rate of 46%. PKEFZ and NKDPZ also demonstrated substantial carbon sequestration capabilities, with the average annual carbon sink of  $0.38 \times 10^8$  t and  $0.22 \times 10^8$  t, respectively. Over the past two decades, the construction land expansion has encroached upon grassland, resulting

in the reduction of carbon sequestration capacity and carbon sink contribution. The ecological land area of the optimized development zone accounted for 51.91% of the Yellow River Basin in 2020. However, the carbon sink contribution rate was only 0.98%, suggesting the poor land carbon carrying capacity and minimal carbon absorption effect in NDOZ (Fig. 4).

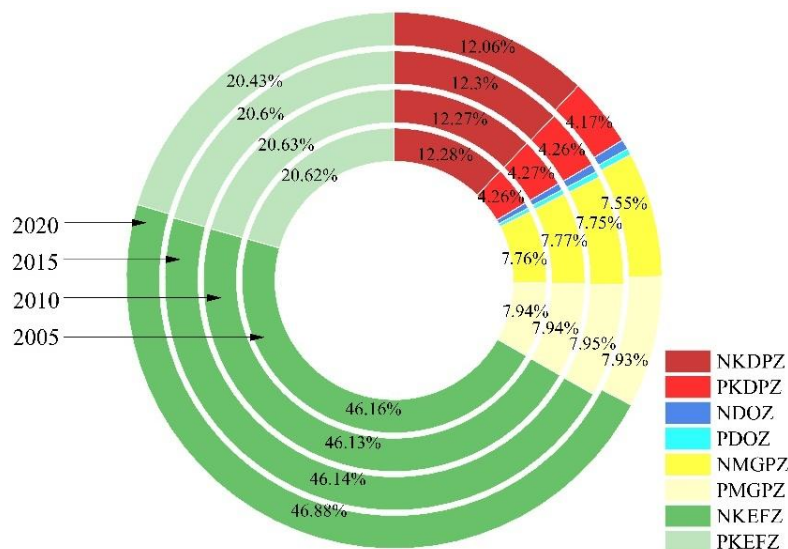


**Figure 4.** Contribution rate of carbon sink for each functional zone in 2005, 2010, 2015 and 2020

#### Net CO<sub>2</sub> emissions

The net CO<sub>2</sub> emissions in 2005, 2010, 2015 and 2020 were  $4.97 \times 10^8$  t,  $8.61 \times 10^8$  t,  $10.97 \times 10^8$  t and  $11.67 \times 10^8$  t, respectively. The CO<sub>2</sub> emissions exhibited an upward trend, which slowed down significantly, and the growth rate was only 5.99% during 2015-2020, indicating that CO<sub>2</sub> emissions will peak around 2030 (Table 5).

**Table 5.** Carbon budget balance in the Yellow River Basin

Years	Direct CO <sub>2</sub> emission/t	Indirect CO <sub>2</sub> emission/t	CO <sub>2</sub> sink/t	Net CO <sub>2</sub> emission/t
2005	$0.04 \times 10^8$	$6.77 \times 10^8$	$-1.84 \times 10^8$	$4.97 \times 10^8$
2010	$-0.02 \times 10^8$	$10.47 \times 10^8$	$-1.84 \times 10^8$	$8.61 \times 10^8$
2015	$0.007 \times 10^8$	$12.81 \times 10^8$	$-1.84 \times 10^8$	$10.97 \times 10^8$
2020	$-0.2 \times 10^8$	$13.74 \times 10^8$	$-1.87 \times 10^8$	$11.67 \times 10^8$

In 2005, approximately 28% of districts and counties in the Yellow River Basin exhibited carbon surplus, mainly located in key ecological function zones (70%). 44.83% of districts and counties exhibited low carbon deficit, primarily concentrated in NMGPZ, where the energy consumption structure remains dominated by coal, agricultural land accounts for approximately 50%, and industrial and agricultural activities have increased CO<sub>2</sub> emissions. In 2010, the number of counties experiencing medium, high and extremely high carbon deficits increased. The carbon deficit counties raised 44 in NMGPZ, and the accompanying net CO<sub>2</sub> emissions increased by  $0.65 \times 10^8$  t. The areas

with high and extremely high carbon deficits are primarily concentrated in regions characterized by resource exploitation and high energy consumption industries, and CO<sub>2</sub> emissions increase by  $0.03 \times 10^8$  t in 2005-2010. The growth rate of net CO<sub>2</sub> emissions in the Yellow River Basin significantly decelerated in 2015, declining from 73.19% in 2005-2010 to 27.42% in 2010-2015. The districts and counties in the optimized development zone have no low-carbon deficit and carbon surplus, while the districts and counties with extremely high carbon deficit exceed 50%, which will greatly increase the difficulty of implementing future energy conservation and emission reduction strategies. In 2020, the growth rate of CO<sub>2</sub> emissions decelerated significantly, while net CO<sub>2</sub> emissions reached peak. From 2005 to 2020 (Fig. 5), counties in PMGPZ are characterized by low CO<sub>2</sub> emissions, without high and extremely high carbon deficit. The county number exhibiting extremely high deficit status decreased or remained unchanged except for NKDPZ, indicating the positive trend in CO<sub>2</sub> emissions in the Yellow River Basin under the implementation of CO<sub>2</sub> emission reduction policies.

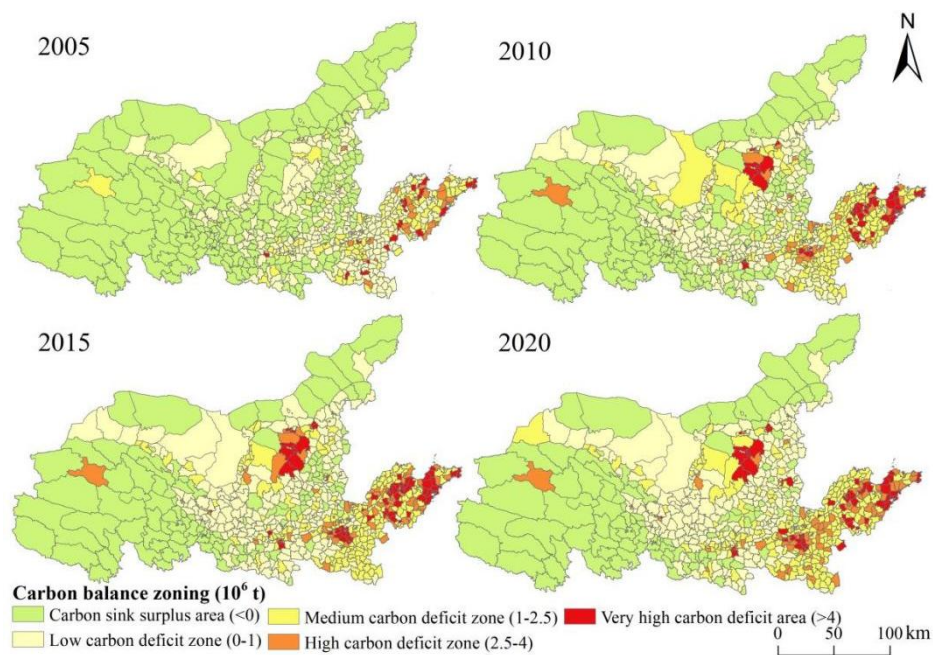


**Figure 5.** Carbon balance zoning of the Yellow River Basin in 2005, 2010, 2015 and 2020

### **Influencing factors of land use net CO<sub>2</sub> emissions**

CO<sub>2</sub> emission is influenced by both natural and human factors. Landscape pattern, vegetation coverage and economic effects of human activities have profound impact on CO<sub>2</sub> emissions in the Yellow River Basin. The main impact factors, including population size (x1), per capita GDP (x2), gross product of secondary industry (x3), energy intensity (x4), energy structure (x5), construction land area (x6), aggregation index (x7) and NDVI (x8), which were selected and classified using discrete processing and the natural breakpoint method, and then were analyzed by geographic detector.

The factor detection shows that the relationship between the interpretation of each factor on net CO<sub>2</sub> emissions in the Yellow River Basin in 2005 is  $x5 > x2 > x1 > x4 > x6 > x3 > x7 > x8$ , which is mainly affected by energy structure, followed by per capita GDP and population. Aggregation index and NDVI contributed little to net CO<sub>2</sub> emission. The

explanatory power of each factor in 2010 was  $x_2 > x_5 > x_1 > x_6 > x_4 > x_3 > x_7 > x_8$ , the impact of per capita GDP was significantly amplified with the  $q$  of 0.34, suggesting the interaction between transform and economic development, and economic growth may lead to more CO<sub>2</sub> emissions. The explanatory power of each factor in 2015 was  $x_5 > x_1 > x_6 > x_4 > x_8 > x_3 > x_8 > x_7$ . Energy structure remains the dominant factor; however, the influence of population has been strengthened, with the  $q$  reaching 0.34. At the same time, the role of construction land has been significantly augmented concurrently with the expansion of human activities, thereby leading to substantial increase in CO<sub>2</sub> emissions. In 2020, the explanatory power of each factor was  $x_5 > x_1 > x_2 > x_6 > x_4 > x_8 > x_3 > x_7$ , and energy structure and population size are the most important, with  $q$  values of 0.29 and 0.14, respectively. Additionally, the significance of GDP of the secondary industry and aggregation index is greater than 0.05, indicating that all factors have comprehensive impact on net CO<sub>2</sub> emissions in 2020, while single factor has weak leading role. Economic factors played predominant role, while natural factors exerted comparatively weaker influence in 2005-2020.

The interaction interpretation of energy structure and construction land is 0.79 in 2005 (Fig. 6). The interaction explanation of per capita GDP and population is 0.74, indicating that economic factors play the pivotal role in CO<sub>2</sub> emissions changes. The interaction explanation between population and per capita GDP is of 0.94 in 2010, indicating the substantial influence of human activities on net CO<sub>2</sub> emissions. The interactive interpretation of construction land with energy intensity and energy structure is 0.83 and 0.84, respectively, signifying that the interaction between construction land and energy factors also greatly affect CO<sub>2</sub> emissions. NDVI exhibits limited explanatory power for CO<sub>2</sub> emissions, whereas its interaction with energy structure reaches 0.69, suggesting that vegetation coverage indirectly influences CO<sub>2</sub> emissions. The explanatory power of per capita GDP and population was 0.95 in 2015. Additionally, the interaction between energy structure and construction land exhibited 0.81. Furthermore, the interactive explanatory degrees of population factor, energy intensity and energy structure were 0.66 and 0.72, respectively, suggesting that population, energy intensity, energy structure and construction land played pivotal roles in influencing CO<sub>2</sub> emissions in 2015. The explanatory power of the aggregation index with population, per capita GDP and energy structure exceeded 0.5. However, the individual factor (aggregation index) did not significantly influence CO<sub>2</sub> emissions, which suggests that the fragmentation degree of land landscape patterns indirectly impacts CO<sub>2</sub> emissions. In 2020, the explanatory power of energy structure with construction land, aggregation index and NDVI was 0.87, 0.81 and 0.83, respectively, indicating that the interaction among energy structure, land landscape and vegetation coverage has stronger impact on CO<sub>2</sub> emissions, and the explanatory power of the interaction between natural factors and social factors is significantly stronger than single factors. The primary drivers of CO<sub>2</sub> emissions have shifted between 2005 and 2020, energy economy and human activities were the predominant factors influencing emissions in 2005-2015, while natural factors and energy economic factors became the leading drivers from 2015 to 2020.

### ***Future projections of carbon budget***

Under the natural development scenario (Fig. 7a), net CO<sub>2</sub> emissions of the Yellow River Basin in 2030 are projected to increase by  $1.36 \times 10^8$  t compared to 2020. About 30% of the districts and counties exhibit carbon surplus, encompassing over 90% of the

river basin. The number of districts and counties in low carbon deficit state remained basically stable, while the number of districts and counties in medium decreased significantly, suggesting the reduction of CO<sub>2</sub> emissions in the Yellow River Basin over the next decade. For different major function-oriented zones, the carbon surplus counties of NMGPZ will increase by 15, while the number of low and medium carbon deficit counties will decrease by 7 and 50, respectively. The opposite trend was observed in PKDPZ, where the number of extremely high carbon deficit counties doubled and CO<sub>2</sub> emissions increased by  $0.64 \times 10^8$  t.

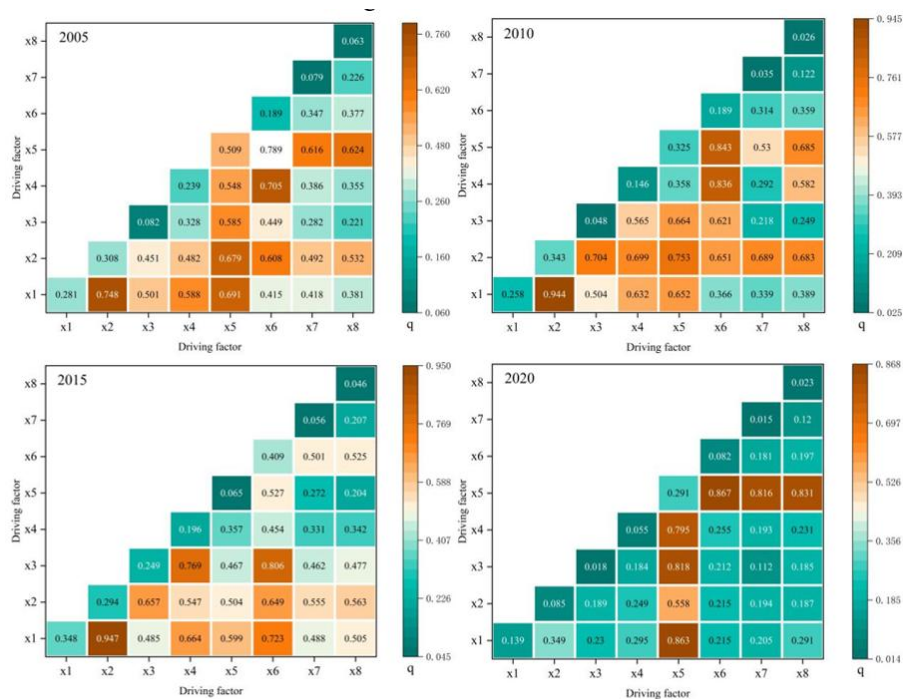


**Figure 6.** Interactive detection of influencing factors for CO<sub>2</sub> emissions in the Yellow River Basin

In the urban expansion scenario (Fig. 7b), net CO<sub>2</sub> emissions peak at  $13.21 \times 10^8$  t in 2030, which is approximately 2.6 times higher than that of 2005, but the growth rate slows down significantly. The number of extremely high carbon deficit counties increased by 18, primarily concentrated in the North China Plain region. In comparison to 2020, CO<sub>2</sub> emissions show consistent decline only in agricultural land, while other functional areas present varying degrees of increase, with the increment of  $1.57 \times 10^8$  t in NKDPZ. In the context of urban expansion, net CO<sub>2</sub> emissions will peak, and high energy consumption is primarily responsible for indirect CO<sub>2</sub> emissions rise. The major grain producing zones with rapid CO<sub>2</sub> emission growth will be crucial areas in future studies.

Due to the substantial population base, the net CO<sub>2</sub> emission amounts to  $12.63 \times 10^8$  t in 2030 under the ecological protection scenario (Fig. 7c), representing the rise of  $0.97 \times 10^8$  tons compared to that of 2020, and the growth rate is consistent with that under the urban expansion scenario, with a significant slowdown. The expansion of carbon sink surplus area will effectively mitigate additional CO<sub>2</sub> emissions. For instance, the carbon sink surplus districts in NKEFZ will increase to 104, grassland serves as the primary land use, with the CO<sub>2</sub> emission reduction of  $0.61 \times 10^8$  t.

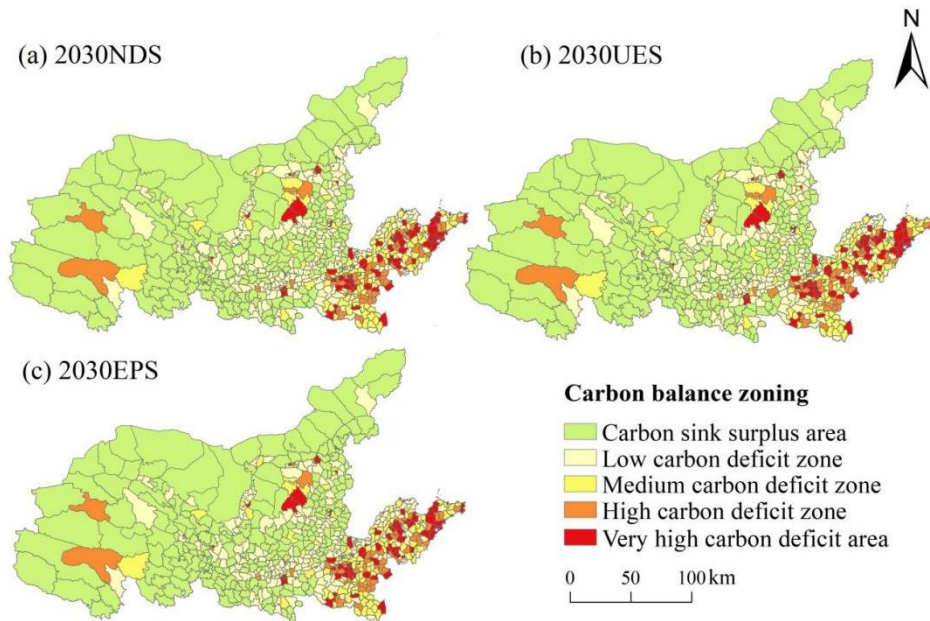


**Figure 7.** Carbon balance zoning in the Yellow River Basin under different scenarios (NDS, UES, EPS) in 2030

## Discussion

### *Recent carbon budget variation in the Yellow River Basin*

In response to global warming, the Chinese government had implemented multiple measures to reduce the carbon emissions. Both carbon emission and carbon sequestration from land use in China had shown a significant increasing trend since 1999 (Zhang et al., 2018; Zhou et al., 2019). As a key region for achieving China's carbon reduction goals, the trend of carbon emission and carbon sequestration in the Yellow River Basin in this study was highly consistent with that of China. In the Yellow River Basin, most of the carbon emissions were concentrated in the central urban agglomeration, while carbon sequestration mainly occurred in the peripheral ecological zones (Ma and Liu, 2021; Yang and Zhen, 2023; Wang and Zhen, 2024). Land use change served as an important factor for carbon emissions. Measures such as returning farmland to forests and improving forest management could promote carbon storage in forests. Reclamation led to the conversion of ecological land into farmland. With the reduction of vegetation and soil carbon storage, the carbon storage of ecosystem decreased, which was a carbon emission process (Ma and Wang, 2015). At present, the carbon budget for the upper, middle and lower reaches of the Yellow River presented obvious disparities. In the upstream, effective carbon emission reduction had been achieved in the Qinghai Province and Inner Mongolia Autonomous Region (Zhang et al., 2018), while the carbon emission intensity from land use increased in the Ningxia Hui Autonomous Region, where the pressure of carbon emission reduction was greater (Zheng and Wen, 2020). In the midstream, the carbon emissions from land use increased in both Shaanxi and Shanxi provinces in recent two decades. Construction land was the main source of carbon emissions, while forests was the main carbon sink (Zhao et al., 2023; Wang et al., 2024). In the downstream, both carbon emission and carbon carrying capacity were not matched spatially in the Henan and Shandong Province, where the carbon deficit was serious (Zhao

2014; Zhang et al., 2018). Most above studies focus on the total carbon emission, which was divided into direct and indirect carbon emission in the current study. The indirect carbon emission had an increasing trend, but the growth rate had decelerated. The direct carbon emission revealed a decreasing trend, hence the effect of natural factors on carbon emission enhancing over time. Further, the functional zone strategy is an important layout of Chinese government to promote regional integration development, constitutes the core strategy to achieve efficient territorial space management. Traditionally, the provincial administrative unit is the policy maker, and the natural zone is the policy implement object. It is difficult to coordinate overall for this strategy, resulting in inefficiency. The targeted policy, implemented in different major function-oriented zoning, is conducive to the optimal allocation of regional resources on carbon emission and sequestration. It provides a new theoretical perspective and scientific basis for accelerating the realization of the carbon budget balance goal.

### ***CO<sub>2</sub> emission reduction countermeasures and suggestions***

Significant disparities exist in the temporal and spatial dynamics of CO<sub>2</sub> emissions and influencing factors among the primary function-oriented zones. Therefore, it is imperative to break the restriction of administrative divisions, formulate spatial planning based on the territorial space development pattern, and implement targeted emission reduction measures for different primary function-oriented zones.

The key development prioritized zones in the Yellow River Basin should (1) enforce stringent CO<sub>2</sub> emission standards and industry access criteria, improve energy efficiency, promote industrial structure upgrade, and the development and application of cleaner production technologies; (2) reveal the potential of land utilization, enhance the utilization efficiency of territorial space, strengthen land intensive use, and mitigate excessive urban expansion (Wang et al., 2020); (3) encourage the development of low-carbon and green industrial parks, and facilitate the green transformation of traditional industries; (4) establish carbon reduction targets to effectively control CO<sub>2</sub> emissions growth in key development zones.

For development optimized zones, it is imperative (1) to prioritize ecological environmental protection and ensure continuous enhancement of resource utilization efficiency; (2) to promote industrial upgrading and green sustainable development, foster technological innovation, and mitigate energy consumption and CO<sub>2</sub> emission intensity; (3) to encourage enterprises to embrace low-carbon technologies and clean energy, and support the development of green buildings and low-carbon transportation.

For the major grain producing zones, it is necessary (1) to reasonably regulate urban expansion, restrict agricultural development activities, and avert the degradation of natural ecosystems resulting from industrialization and urbanization; (2) to improve environmental quality through intensify degree increase, cultivated land protection, and mitigating excessive land occupation and resource exploitation; (3) to prioritize agricultural science and technology innovation, elevate the efficiency and technical of cultivated land, and ultimately achieve agricultural modernization (Wu et al., 2021).

The enhancement of ecosystem services should be prioritized for key ecological function zones. By enhancing the quantity and quality of ecological products, expanding green ecological space, and bolstering carbon sequestration capacity, the ecological balance and ecosystem health is ensured. Strictly control large-scale, high-intensity development activities and prohibit the establishment of industries with high pollution and energy consumption. In the future carbon trading market, the area should the

compensation role of key ecological function zones for ecological construction, restoration and protection should be fully utilized to provide new development opportunities (Wang and Zhen, 2024).

## Conclusions

From the viewpoint of primary function-oriented zoning, the study analysed the spatiotemporal differentiation of carbon budget in each functional zone, investigated the influence of natural and social factors on CO<sub>2</sub> emissions using geographic detection techniques, predict the future dynamics of net CO<sub>2</sub> emissions under various scenarios using CA-Markov model, and proposed CO<sub>2</sub> emission reduction measures and suggestions for the Yellow River Basin. The direct CO<sub>2</sub> emissions revealed the declining trend, carbon sink areas increased, carbon carrying capacity enhanced, and the growth rate of CO<sub>2</sub> emissions significantly decelerated. The factor detection indicated that the impact of individual factors on LULC net CO<sub>2</sub> emissions from was generally limited, whereas the influence of energy structure and per capita GDP surpassed that of natural factors. The interaction detection indicates that the net CO<sub>2</sub> emissions are primarily influenced by the interplay of energy economy and human activities in 2005-2015, while the dominant factor shifts to the interaction between natural factors and energy economy in 2015-2020. In order to accomplish "carbon neutrality" and "carbon peaking", it is imperative to further optimize the measures for diverse functional areas in the future and put forward more constructive recommendations. This study has important reality significance for the planning of primary function-oriented zones and the realization of carbon budget balance in the Yellow River Basin, and can also provide scientific reference for the implementation of "carbon neutrality" policy and sustainable development in resource-based areas with high energy consumption worldwide.

**Conflict of interest.** All authors certify that they have no affiliations with or involvement in any organization or entity with any financial interest or non-financial interest in the subject matter or materials discussed in this manuscript.

**Author contributions.** Wang Sheng: Conceptualization, Investigation, Project administration, Supervision, Validation, Writing—review & editing. Li Dan: Data curation, Formal analysis, Methodology, Software, Writing—original draft preparation. Li Xiujuan: Conceptualization, Formal analysis, Methodology, Resources, Supervision, Visualization. Li Lingfeng: Writing—original draft preparation, Formal analysis, Methodology. Li Qing: Data curation, Writing—review & editing. Wang Jinfeng: Formal analysis, Investigation, Writing—review & editing.

**Acknowledgments.** This project was supported by the National Key Research and Development Program of China (2023YFF1305304); National Natural Science Foundation of China (42401042); Science Technology Project of Hebei Academy of Sciences (25A14); Science and Technology Strategy Project of Shanxi Province (202404030401113, 202304031401073); Basic Research Program of Shanxi Province (202203021211258).

## REFERENCES

- [1] Alam, S. A., Starr, M., Dixon, R. (2013): Tree biomass and soil organic carbon densities across the Sudanese woodland savannah: A regional carbon sequestration study. – *Journal of Arid Environments* 89: 67-76.

- [2] Aleinikovas, M., Jasinevičius, G., Škėma, M., Beniusiene, L., Silinskas, B., Varnagiryte, L. (2018): Assessing the effects of accounting methods for carbon storage in harvested wood products on the national carbon budget of Lithuania. – *Forests* 9: 737.
- [3] Assis, T. O., Aguiar, A. P. D., Randow, C. V., Nobre, C. (2022): Projections of future forest degradation and CO<sub>2</sub> emissions for the Brazilian Amazon. – *Science Advances* 8: 24.
- [4] Buendia, L., Eggleston, S., Miwa, K. et al. (2006): 2006 IPCC guidelines for national greenhouse gas inventories. Tokyo: Preparation of the National Greenhouse Gas Inventories Plan. – IPCC, International Panel on Climate Change.
- [5] Caute, H., Lawrence, W. M. A. (2017): Markovian and cellular automata land use change predictive model of the Usangu Catchment. – *International Journal of Remote Sensing* 38: 64-81.
- [6] Chang, X. Q., Xing, Y. Q., Wang, J. Q., Yang, H., Gong, W. S. (2022): Effects of land use and cover change (LULC) on terrestrial carbon stocks in China between 2000 and 2018. – *Resources, Conservation and Recycling* 182: 106333.
- [7] Chen, G. S., Yang, Y. S., Liu, L. Z., Li, X. B., Zhao, Y. C., Yuan, Y. D. (2007): Research review on total below ground carbon allocation in Forest Ecosystems. – *Journal of Subtropical Resources and Environment* 1: 34-42.
- [8] Fan, J., Tao, A. J., Ren, Q. (2010): On the Historical Background, Scientific Intentions, Goal Orientation, and Policy Framework of Major Function-Oriented Zone Planning in China. – *Journal of Resources and Ecology* 1: 289-299.
- [9] Fan, J. (2015): Draft of major function oriented zoning of China. – *Acta Geographica Sinica* 70: 186-201.
- [10] Fan, J. S., Yu, X. F., Zhou, L. (2018): Carbon emission efficiency growth of land use structure and its spatial correlation: A case study of Nanjing city. – *Geographical Research* 37: 2177-2192.
- [11] Gatti, L. V., Basso, L. S., Miller, J. B., Gloor, M., Domingues, L. C., Cassol, H., Tejada, G., Aragao, L., Nobre, G., Peters, W., Marani, L., Arai, E., Sanches, A., Correa, S. M., Anderson, L., Randow, C. V., Correia, C., Crispim, S., Neves, R. A. (2021): Amazonia as a carbon source linked to deforestation and climate change. – *Nature* 595: 388-393.
- [12] Giardina, C. P., Ryan, M. G. (2000): Evidence that decomposition rates of organic carbon in mineral soil do not vary with temperature. – *Nature* 404: 858-61.
- [13] Huang, Z. X., Pan, B. (2020): Progress, Problems and Suggestions on the Implementation of Main Functional Area Planning. – *Natural Resource Economics of China* 33: 4-9.
- [14] Huang, X. J., Zhang, X. Y., Lu, X. H., Wang, P. Y., Qin, J. Y., Jiang, C. Y., Liu, Z. M., Wang, Z., Zhu, A. X. (2021): Land development and utilization for carbon neutralization. – *Journal of Natural Resources* 36: 2995-3006.
- [15] Hussin, F., Aroua, M. K., Kassim, M. A., Ali, U. F. M. (2021): Transforming Plastic Waste into Porous Carbon for Capturing Carbon Dioxide: A Review. – *Energies* 14: 1-22.
- [16] IPCC. (2021): *Climate Change 2021: The Physical Science Basis*. – Cambridge University Press, International Panel on Climate Change.
- [17] Jayakrishnan, K. U., Bala, G., Cao, L., Caldeira, K. (2022): Contrasting climate and carbon-cycle consequences of fossil-fuel use versus deforestation disturbance. – *Environmental Research Letters* 17: 064020.
- [18] Jin, Z., Wang, T., Zhang, H. Q., Wang, Y. L., Ding, J. Z., Tian, X. J. (2023): Constraint of satellite CO<sub>2</sub> retrieval on the global carbon cycle from a Chinese atmospheric inversion system. – *Science China Earth Sciences* 53: 587-597.
- [19] Li, L., Xia, Q. Y., Dong, J., Zhang, B. (2023): County-level carbon ecological compensation of Wuhan Urban Agglomeration under carbon neutrality target: based on the difference in land use carbon budget. – *Acta Ecologica Sinica* 43: 2627-2639.
- [20] Ma, X. Z., Wang, Z. (2015): Progress in the study on the impact of land-use change on regional carbon sources and sinks. – *Acta Ecologica Sinica* 35: 5898-5907.

- [21] Ma, Y., Liu, Z. Z. (2021): Study on the spatial-temporal evolution and influencing factors of land use carbon emissions in the Yellow River Basin. – *Ecological Economy* 37(7): 35-43.
- [22] Mi, Z. F., Zheng, J. L., Meng, J., Zheng, H. R., Li, X., Coffman, D., Woltjer, J., Wang, S. Y., Guan, D. B. (2019): Carbon emissions of cities from a consumption-based perspective. – *Applied Energy* 235: 509-518.
- [23] Pan, J. H., Zhang, Y. N. (2021): Spatiotemporal patterns of energy carbon footprint and decoupling effect in China. – *Acta Geographica Sinica* 76: 206-222.
- [24] Ploeg, F. V. D., Withagen, C. (2012): Is there really a green paradox? – *Journal of Environmental Economics and Management* 64: 342-363.
- [25] Quéré, C. L., Andrew, R. M., Friedlingstein, P. et al. (2018): Global carbon budget 2018. – *Earth System Scientific Data* 10(4): 2141-2194. doi:10.5194/essd-10-2141-2018.
- [26] Ran, C., Bai, X. Y., Tan, Q., Luo, G. J., Cao, Y., Wu, L. H., Chen, F., Li, C. J., Luo, X. L., Liu, M., Zhang, S. R. (2023): Threat of soil formation rate to health of karst ecosystem. – *Science of the Total Environment* 887: 163911.
- [27] Strengthening Action on Climate Change (2015): China's Nationally Determined Contribution (Full Text). – 2015-06-30. [https://www.gov.cn/xinwen/2015-06/30/content\\_2887330.htm](https://www.gov.cn/xinwen/2015-06/30/content_2887330.htm).
- [28] Syphard, A. D., Clarke, K. C., Franklin, J. (2005): Using a cellular automaton model to forecast the effects of urban growth on habitat pattern in southern California. – *Ecological Complexity* 2: 185-203.
- [29] Walsh, J. J. (2001): Importance of continental margins in the marine biogeochemical cycling of carbon and nitrogen. – *Nature* 350: 53-55.
- [30] Wang, J. F., Li, X. H., Christakos, G., Liao, Y. L., Zhang, T., Gu, X., Zheng, X. Y. (2010): Geographical detectors-based health risk assessment and its application in the neural tube defects study of the Heshun region, China. – *International Journal of Geographical Information Science* 24: 107-127.
- [31] Wang, J. F., Hu, Y. (2012): Environmental health risk detection with Geog Detector. – *Environmental Modelling & Software* 33: 114-115.
- [32] Wang, J. F., Xu, C. D. (2017): Geodetector: Principle and prospective. – *Acta Geographica Sinica* 72: 116-134.
- [33] Wang, L. G., Ding, C. X., Peng, J. F., Li, W. M. (2020): Comparison of factors affecting tourism operators' carbon offset willingness of forest parks. – *Economic Geography* 40(5): 230-238.
- [34] Wang, T., Zhao, R., Yin, Y., Deng, L. J. (2023): Accounting Method of Greenhouse Gas Absorption and Emission in Coastal Wetland. – *Statistics Decision* 39: 56-60.
- [35] Wang, S. Y., Li, Y., Yang, J. Y., Yu, E., Lei, K. G., Feng, X. H. (2023): Land Use Change Driving and Optimization of Carbon Budget in Hangzhou Metropolitan Area. – *Environmental Science and Pollution Research* 10: 1-18.
- [36] Wang, Y. Q., Zhen, W. Q. (2024): Spatio-temporal Differentiation of Carbon Budget and Carbon Compensation Zoning Based on the Plan for Major Function-oriented Zones: A Case Study of Counties in the Yellow River Basin. – *Environmental Science* 45(09): 5015-5026.
- [37] Wang, J. F., Li, Y., Wang, S., Li, Q., Wang, R. D., Zhang, R., Ge, X. (2024): Evolution and driving mechanism of multiple ecosystem services in resource-based region of northern China. – *Scientific Reports* 14: 22338.
- [38] Wu, G. Y., Liu, J. D., Yang, L. S. (2021): Dynamic evolution of China's agricultural carbon emission intensity and carbon offset potential. – *China Population, Resources and Environment* 31(10): 69-78.
- [39] Xi, J. P. (2020): Build on past achievements and embark on a new journey for the global response to climate change. – *People's Daily*. 2020-12-13(002).

- [40] Xia, S. Y., Yang, Y. (2022): Spatio-temporal differentiation of carbon budget and carbon compensation zoning in Beijing-Tianjin-Hebei Urban Agglomeration based on the Plan for Major Function-oriented Zones. – *Acta Geographica Sinica* 77: 679-696.
- [41] Xu, R., Huang, X. J., Wang, P. Y., Liu, Z. M., Liang, J., Yang, L., Zhang, X. Y. (2022): Territorial spatial carbon neutrality realization degree of the Yellow River: A case study of the Inner Mongolia section. – *Acta Ecologica Sinica* 42: 9651-9662.
- [42] Yang, F., Zhen, J. H. (2023): Relationship between Pollution and Carbon Reduction and Economic Growth in Typical Regions under the 'Dual Carbon' Goals: A Case Study of Urban Agglomeration in the Yellow River Basin. – *Research of Environmental Sciences* 36: 2050-2064.
- [43] Zhang, P. Y., He, J. J., Hong, X., Zhang, W., Qin, C. Z., Pang, B., Li, Y. Y., Liu, Y. (2018): Carbon sources/sinks analysis of land use changes in China based on data envelopment analysis. – *Journal of Cleaner Production* 204: 702-711.
- [44] Zhao, R. Q., Zhang, S., Huang, X. J., Qin, Y. C., Liu, Y., Ding, M. L., Jiao, S. X. (2014): Spatial variation of carbon budget and carbon balance zoning of Central Plains Economic Region at county-level. – *Acta Geographica Sinica* 269(10): 1425-1437.
- [45] Zhao, R. Q., Huang, X. J., Chai, X. W. (2016): Misunderstandings and Future Trends of Researches on Land Use Carbon Emissions in China. – *China Land Science* 30: 83-92.
- [46] Zhao, C. X., Liu, Y. L., Yan, Z. X. (2023): Effects of land-use change on carbon emission and its driving factors in Shaanxi Province from 2000 to 2020. – *Environmental Science and Pollution Research* 30: 68313-68326.
- [47] Zheng, Y. C., Wen, Q. (2020): Change of Land Use and the Carbon Emission Effect of Ningxia Autonomous Region. – *Journal of Soil and Water Conservation* 27: 207-212.
- [48] Zhou, J., Wang, Y. X., Liu, X. R., Shi, X. C., Cai, C. M. (2019): Spatial Temporal Differences of Carbon Emissions and Carbon Compensation in China Based on Land Use Change. – *Journal of Geographical Sciences* 39: 1955-1961.
- [49] Zhou, L., Dang, X. W., Sun, Q. K., Wang, S. H. (2020): Multi-scenario simulation of urban land change in Shanghai by random forest and CA-Markov model. – *Sustainable Cities and Society* 55: 102045.